IMEKO 23rd TC3, 13th TC5 and 4th TC22 International Conference
30 May to 1 June, 2017, Helsinki, Finland

INVESTIGATION OF IMPACT HAMMER CALIBRATIONS

M. Kobusch [1], L. Klaus [1], and L. Muñiz Mendoza [2]

[1] Physikalisch-Technische Bundesanstalt (PTB), Bundesallee 100, 38116 Braunschweig, Germany, michael.kobusch@ptb.de
[2] Centro Nacional de Metrología (CENAM), km 4.5 Carretera a Los Cués, Municipio El Marques, Querétaro, C.P. 76246, México

Abstract: This paper presents recent theoretical and experimental investigations of calibration measurements of impact hammers using different dynamic calibration set-ups with primary traceability methods. In the scope of a scientific collaboration between the German national metrology institute PTB and the Mexican CENAM, measurements of selected hammers were conducted at both institutes. The analysis of the measurement signals in the time and frequency domain is presented and discussed.

Keywords: Modal hammer, dynamic calibration, shock force, sensitivity.

1. INTRODUCTION

Impact hammers (or modal hammers) are a widely used handheld tool in science and industry for the modal testing (or experimental modal analysis) of mechanical components and interconnected mechanical structures. The instrumented hammers feature an integrated force transducer to measure the dynamic force stimulus that excites the mechanical structure under test. The main purpose of these experimental tests is the determination of the test structure's impulse responses, mode shapes, resonances, and damping by means of additional acceleration sensors which pick up the shock response at specific points of interest [1].

The appropriate calibration of impact hammers has gained importance in order to satisfy measurement accuracy demands and the needs of the quality management employed. Considering the related mechanical transducers for acceleration and force, it is well known that these transducers show a frequency-dependent response which basically depends on their mechanical design and the mechanical coupling to the environment. Consequently, the establishment of traceable calibrations of impact hammers has become a topic of recent research activities at the national metrology institute (NMI) level. In the scope of a scientific collaboration between the German national metrology institute PTB and the Mexican CENAM, methods for the primary calibration of impact hammers have been investigated at both institutes.

This paper presents dynamic calibration measurements of a selected impact hammer specimen conducted at the experimental calibration set-ups of both institutes. A hammer stroke generates an approximately half-sine-shaped force pulse of short duration. The dynamic output signal of the impact hammer is then compared to a measured reference force, which is the inertia force of a known reaction mass body at which the hammer impacts. The experimental challenges in measurement and data analysis, considering the time and the frequency domain, are introduced and discussed in the following.

2. MEASUREMENT PRINCIPLE

The current research activities focus on dynamic calibrations following primary methods for the traceable measurement of the hammer force pulse. The reference force is determined as the product of the mass and acceleration of the reaction mass body, with the mass value obtained by weighing, and the time-dependent acceleration determined by an acceleration measurement. Figure 1 illustrates the principle of the dynamic impact hammer calibration.

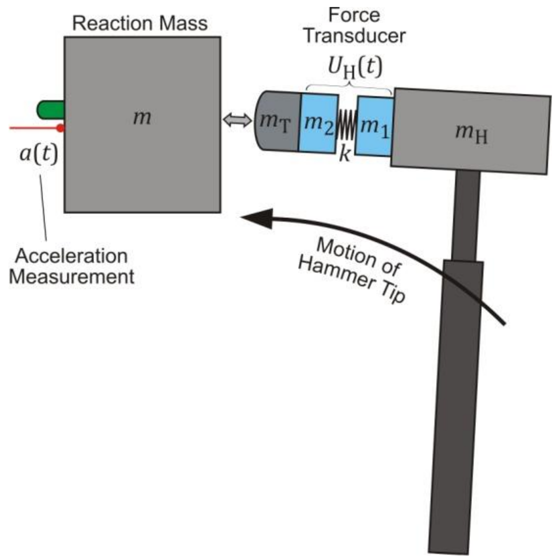

Figure 1. Model of the impact hammer calibration.

The hammer strikes the reaction mass m, and its time-dependent course of acceleration $a(t)$ is picked up at the opposing body face by an attached acceleration sensor (marked in green) or by a contactless beam of a laser vibrometer (red). Both dynamic signals, the hammer's force transducer output $U_H(t)$ and the acceleration $a(t)$, are recorded with a sufficiently high sampling rate.

The figure further illustrates the basic model to describe the dynamic behaviour of the calibration set-up. The mechanical structure is modelled by a lumped mass model, i.e. a series arrangement of spring-coupled rigid mass bodies. In accordance with the dynamic modelling of force transducers [2], the hammer's integrated force transducer is described by two parts (masses m_1, m_2) coupled by an elastic spring (stiffness k) and connected to the hammer tip and the hammer mass, respectively. The hammer signal $U_H(t)$ is assumed to be proportional to the spring compression.

The magnitude and duration of the force pulses can be varied by applying differently strong hammer strokes and by using hammer tips of different hardness. Figure 2 shows typical hammer signals in the time and frequency domain which were obtained with different hammer tips. For a given impact magnitude of the applied hammer stroke, i.e. the momentum defined as the product of the hammer mass and impact velocity, soft hammer tips generate long pulses of small force amplitude, and hard tips short pulses of large amplitude. In the frequency domain, long pulses correspond to lower frequency contents, and short pulses to higher frequency contents.

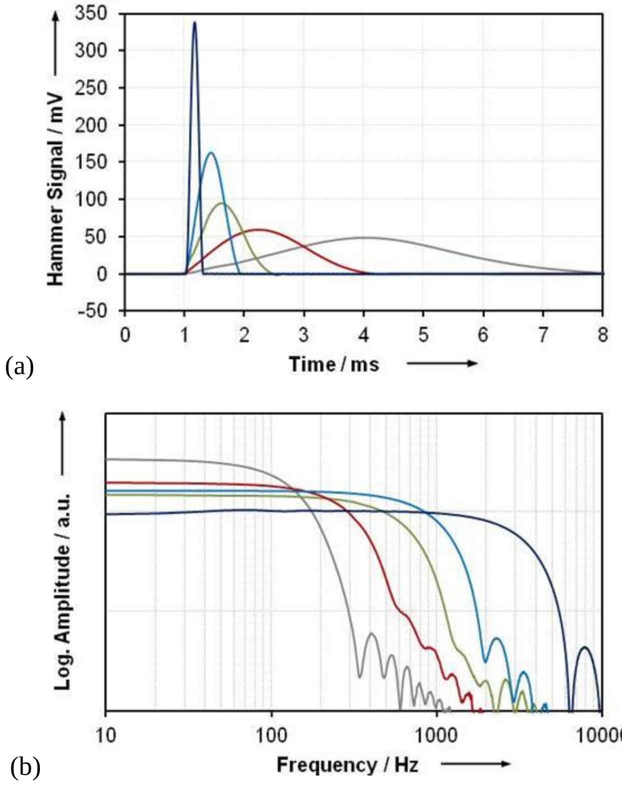

Figure 2. Hammer signals measured with five different hammer tips in the time (a) and frequency (b) domain.

The calibration set-ups realized at PTB and CENAM use reaction mass bodies (various mass values available) which are either suspended by strings (pendulum arrangement) or guided by an air bearing to assure a defined axial motion with low friction. Figure 3 visualizes the principal motion of the hammer-excited reaction mass body for three different arrangements. Considering a pendulum suspended at both ends with one common pivot point, the mass performs a rotational motion which results in a radial distribution of acceleration at the front surface. In the case of a string geometry with two pivot points, the pendulum shows a parallelogram-type motion with an even acceleration over its front surface. This geometry however exhibits a transversal motion component. In order to guarantee a linear motion without parasitic rotational and transversal components, a linear air bearing is further investigated. This linear motion is advantageous compared to the pendulum designs, but the costs of purchase are considerably higher and will thus limit its versatility, as modifications of the set-up are barely possible.

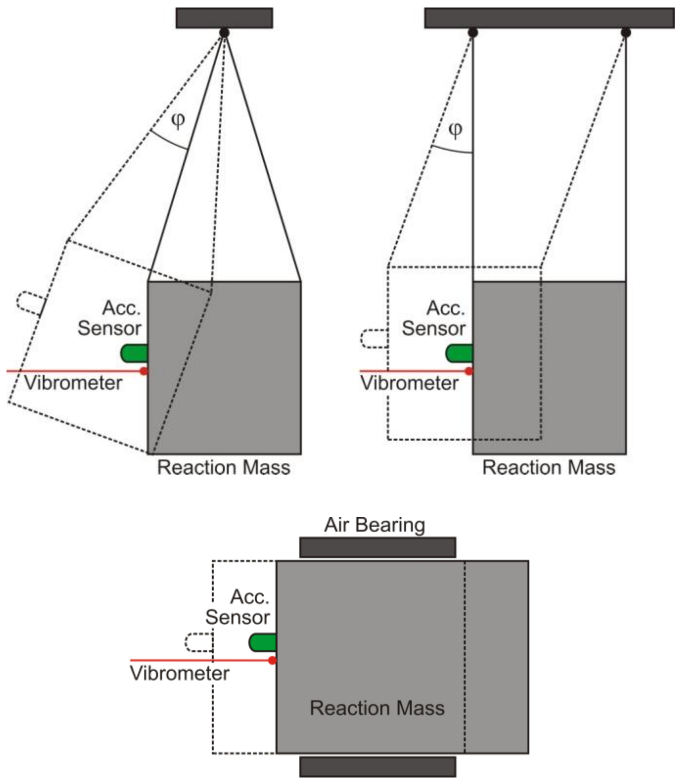

Figure 3. Calibration set-ups using a pendulum (top) and an airborne (bottom) reaction mass body.

Regarding the repeatability in measurement, it has to be noted that an impact hammer is a handheld instrument, and the user-dependent test conditions may affect the calibration results. The variability of manually guided hammer strokes includes the applied momentum, the curved hammer motion, the location and direction of the impact force, as well as the mechanical interaction with the operator's arm. Although these influences might be negligible, the great variability is a challenge for well-defined calibration conditions.

Impact hammers are commonly equipped with a piezoelectric force transducer of high stiffness, and therefore, of high bandwidth. Dynamic effects due to inertia forces of the hammer's mechanical structure are assumed to be small. However, the shock pulses might be very short and dynamic effects due to inertia forces of the particular calibration set-up, i.e. from the reaction mass, the hammer tips, or the hammer mass, should not be generally ruled out. Whereas these effects may be correctly modelled by the dynamic model sketched in Figure 1, parasitic vibrations from shock-excited modal vibrations, which could be observed at the shock force calibration devices [2], will not be described.

In general, it is necessary to know and compensate for the dynamic behaviour of both signal measuring chains in the frequency range of interest. This consideration includes the measuring amplifiers and signal conditioners [3], the data acquisition electronics as well as the data processing software. Whereas dedicated charge amplifiers can be calibrated prior to the calibration measurements, an appropriate compensation is not possible in the case of force or acceleration sensors with integrated electronics, the so-called IEPE (Integrated Electronics Piezoelectric) sensors.

3. SIGNAL ANALYSIS

The impact hammer calibration measurements are based on the analysis of two pulse-shaped signals, the hammer output $U_H(t)$ and the acceleration $a(t)$ of the reaction mass m which gives the reference force $F(t) = m \cdot a(t)$. The signal ratio U_H / F then leads to the sought calibration result, the shock sensitivity S_{sh}. Figure 4 illustrates the two principal methods of the signal analysis in the time and frequency domain.

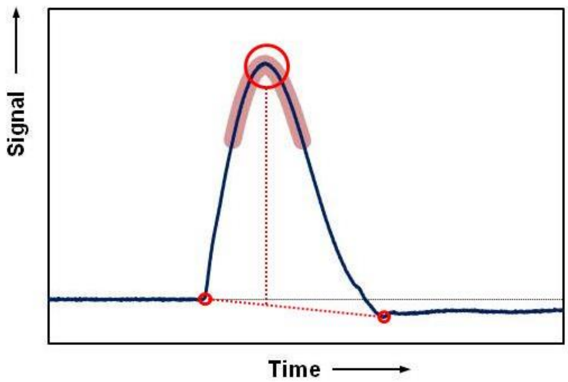

(a)

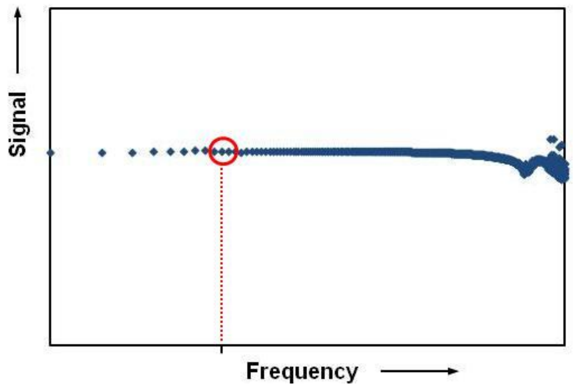

(b)

Figure 4. Signal analysis in the time domain (a) and frequency domain (b).

Considering a signal analysis in the time domain (Figure 4a), shock calibration results are typically based on the evaluation of pulse peak ratios. To suppress affecting signal noise, the pulse peak values may be determined by a peak fitting procedure. In the case of a high-pass characteristic of the measurement instrumentation, which is always the case for a piezoelectric sensor, ground level offsets may be corrected by a trapezoidal correction if necessary [4]. For a set of calibration measurements with varying pulse heights, the shock sensitivity can be calculated as the averaged pulse peak ratio of each individual hammer pulse, or can be determined by a linear regression of the hammer and acceleration peak values (cf. Figure 9).

Modal testing with impact hammer excitations usually analyses spectral measurement data. The spectral range of the force excitation is an important criterion (cf. Figure 2). In this regard, it is useful to directly specify the sensitivity of the hammer output from frequency domain data (Figure 4b). Here, the shock sensitivity can be expressed as the ratio of the spectral amplitude values at a specific frequency, e.g. at 100 Hz.

4. EXPERIMENTAL MEASUREMENTS

Within the scope of a scientific collaboration between the German and the Mexican NMIs, calibration measurements of impact hammers have been conducted at both institutes to investigate the procedures and methods and to obtain a first comparison of calibration results. The different experimental dynamic calibration set-ups are shown in Figure 5.

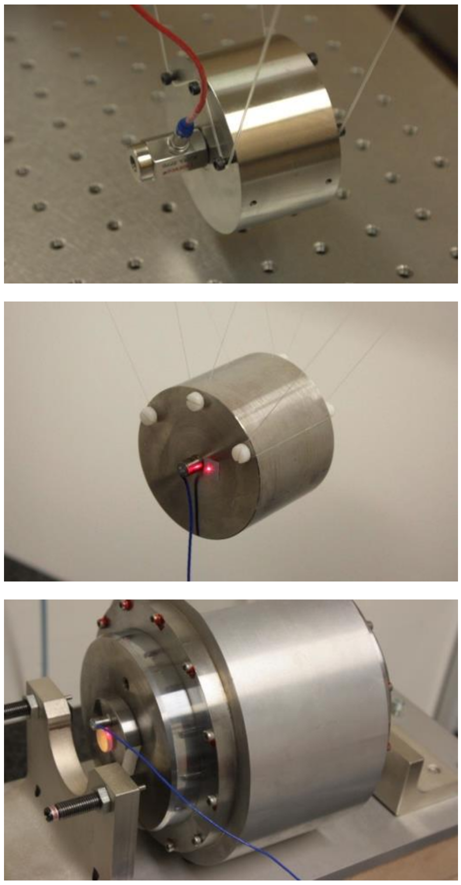

Figure 5. Impact hammer calibration set-ups applying a pendulum mass at CENAM (top), at PTB (centre), and an airborne mass body at PTB (bottom).

At CENAM, the impact hammer calibration set-up used two differently sized pendulum masses made of stainless steel and an accelerometer (Endevco 2270) which was axially mounted via a threaded stud bolt. The total mass of these reaction masses amounted to 0.77 kg and 1.47 kg, respectively. The measurement instrumentation further consisted of a charge amplifier (Brüel & Kjær 2635) and a data acquisition and IEPE conditioning system (National Instruments PXI-4461).

At PTB, impact hammer calibration measurements were conducted with a pendulum mass of 1.0 kg and an airborne mass of 8.2 kg. In both cases, the acceleration of the reaction mass was obtained by a laser vibrometer (Polytec OFV 503) and an acceleration sensor (PCB 352B10) glued at the front surface. The instrumentation further consisted of a charge amplifier (Kistler type 4011), an IEPE conditioner (PCB Piezotronics 482C series), and a data acquisition system (National Instruments PXI-5124, PXI-5922).

The experimental tests and results given in the following are only to be considered as examples to adequately describe the investigated methods and procedures of an impact hammer calibration. All the measurements presented in this paper were conducted with a Kistler 9726A20000 impact hammer. The selected hammer applies an IEPE sensor of 20 kN force range, features a hammer head of 500 g, and can be equipped with five interchangeable hammer tips of different hardness.

Figure 6 shows the pulse parameters measured with a Kistler 9726A20000 impact hammer using five differently stiff hammer tips for a set of 26 individual measurements each. The experimental tests showed that the pulse width slightly decreases for stronger hammer strokes, which results from a nonlinear contact stiffness of the hammer tip. A dependence on the operator was not observed.

A corresponding spectral analysis of these 130 pulses is given in Figure 7, showing the averaged amplitudes of the shock sensitivity for each of the five hammer tips. At low frequencies, the sensitivities obtained with the two hardest tips (steel, plastic) obviously differ from those with the three softest ones (rubber), which clearly indicates that dynamic effects from the inertia force of the hammer tip might be seen. The directly screwed hardest tips have a mass of about 2 g, and the softer tips use an adapter which results in a much higher mass of about 37 g.

Simultaneous measurements with an acceleration sensor and a laser vibrometer demonstrate that the motion should be preferably measured at the surface centre to minimize influences from modal vibrations (bending modes) and, in particular, from low-frequent oscillations of the reaction mass, which will be excited by oblique or non-centric hammer strokes. In this context, a low-frequent ringing was commonly observed for soft hammer tips, i.e. long shock pulses, and for a mass suspension (or guidance) of comparably higher lateral stiffness, e.g. at the airborne 8 kg reaction mass.

Furthermore, the calibration measurements obtained with the hammer tips made of rubber demonstrate that the impacting surfaces experience some kind of sticking effect, as the rebounding impact hammer measures a small tension force when the shock pulse ends.

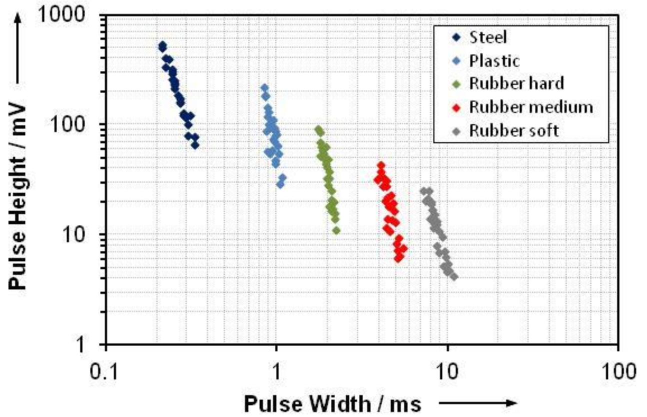

Figure 6. Pulse parameters achieved with a Kistler 9726A20000 impact hammer for five hammer tips of different materials, 26 pulses each, measured at CENAM using a pendulum mass of 1.47 kg.

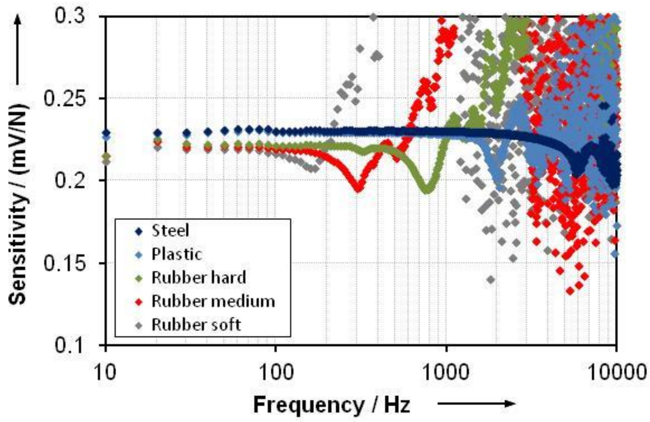

Figure 7. Spectral sensitivity for five hammer tips, average of 26 pulses each, measured at CENAM.

In general, short pulses obtained with the hard hammer tips significantly excite modal resonances of the reaction mass, the hammer, and the acceleration sensor. This “noise” has to be appropriately low-pass filtered for an analysis in the time domain. Figure 8 gives an example demonstrating the importance of this filtering and shows the two acceleration signals measured at the airborne mass body with an impact hammer excitation using the steel tip. The signals filtered by a low-pass filter of 100 kHz cut-off frequency are dominated by modal oscillations. A 15 kHz low pass (Bessel, 8th order) was needed to suppress the strongest noise components in order to obtain a smooth pulse. This signal still exhibits a small ringing of about 18 kHz, which belongs to the first longitudinal resonance of the mass body.

A first comparison of the results of the calibration measurements conducted at PTB and CENAM is presented in Figure 9. The analysis of the shock pulse data of the impact hammer selected as an example was performed in the time domain. The diagram shows the distribution of the measured pulse peak values of the reference force and the hammer output for hammer strokes obtained with the steel tip, about 50 data points of each institute. A linear regression finally gives the averaged pulse peak ratio, i.e. the shock sensitivity to be determined. The calibration results of 0.222 mV/N (PTB) and 0.219 mV/N (CENAM) deviate by only 1 % and agree with the specified nominal sensitivity of 1 mV/lbf (0.225 mV/N).

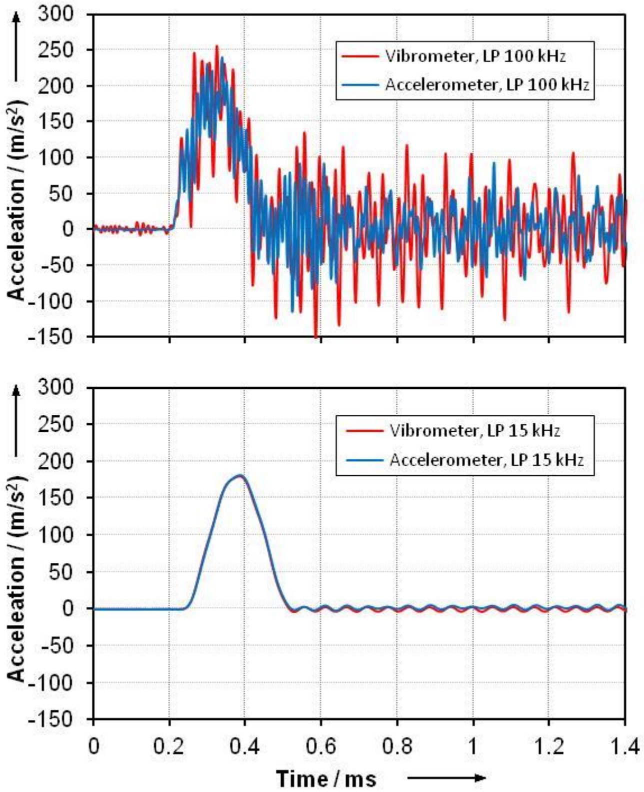

Figure 8. Filtering of the noisy acceleration signals using different low-pass (LP) filters, impact hammer with steel tip, measured at PTB's airborne reaction mass of 8 kg.

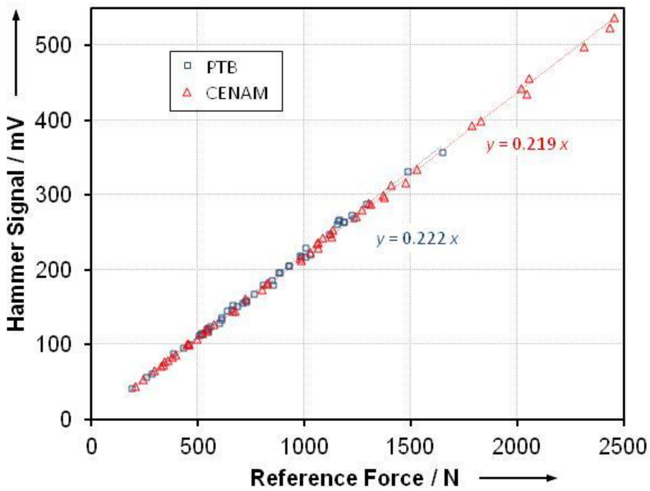

Figure 9. Comparison of the pulse peak values measured at PTB and CENAM: Kistler 9726A20000 impact hammer with steel tip; the gradient determined by a linear regression represents the shock sensitivity of the hammer.

5. DISCUSSION AND CONCLUSIONS

This paper presents investigations of impact hammer calibration measurements conducted within the scope of a scientific collaboration between PTB and CENAM. It was found that the different set-ups may give consistent results. The calibration results obtained at both institutes could be compared for the first time. For the impact hammer tested as an example, the measured shock sensitivities deviate in the order of 1 %.

However, some parasitic influences from the mechanical set-up or the experimental test conditions could be observed, which may affect the calibration results. Hammer tips of different mass and stiffness gave slightly different shock sensitivities, probably due to dynamic effects within the hammer head. In addition, considerably strong disturbances resulted from modal vibrations of the shock-excited reaction mass body and the accelerometer. In particular for short pulses of high frequency content, the appropriate filtering or minimization of parasitic modal vibrations is very important for the pulse analysis in the time domain. The resonances of the reaction mass body on which the impact hammer strikes should be as high as possible, in order to achieve a broad calibration bandwidth.

For this purpose, the modal vibrations of a cylindrical reaction mass were investigated by a finite element (FE) modal analysis. Considering a steel body of 1 kg mass and 60 mm diameter, its two lowest longitudinal modes are found at about 45 kHz (Figure 10). These modes represent the axisymmetric in-phase (left) and out-of-phase vibration of the cylinder end faces, respectively. Definitely excited by the hammer strokes, the longitudinal vibration modes will set the limits to the useable bandwidth of the acceleration measurement that provides the reference force signal. In contrast, parasitic influences from other modal vibrations, e.g. non-axisymmetric bending modes, which may even appear at lower frequencies, are suspected to be much smaller and may be neglected if the acceleration is sensed at the body axis. To find the best geometrical shape of the cylindrical body, the influence of the aspect ratio (ratio of length to diameter) is shown in Figure 11. The diagram visualizes the modal frequencies of the first two longitudinal modes as well as of the lowest resonance, which is either plate bending, torsion or rod bending. The highest modal frequencies can be expected for an aspect ratio of about 0.8.

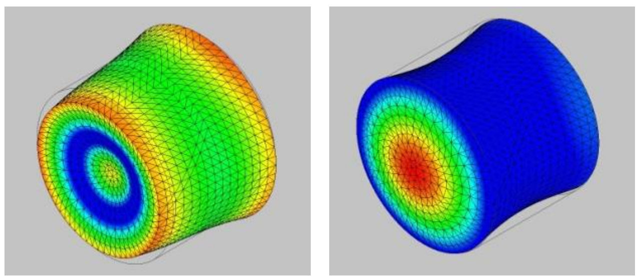

Figure 10. FE calculation of the first two longitudinal modes at 44.2 kHz (left) and 46.2 kHz of a 1 kg cylinder made of steel with a diameter of 60 mm.

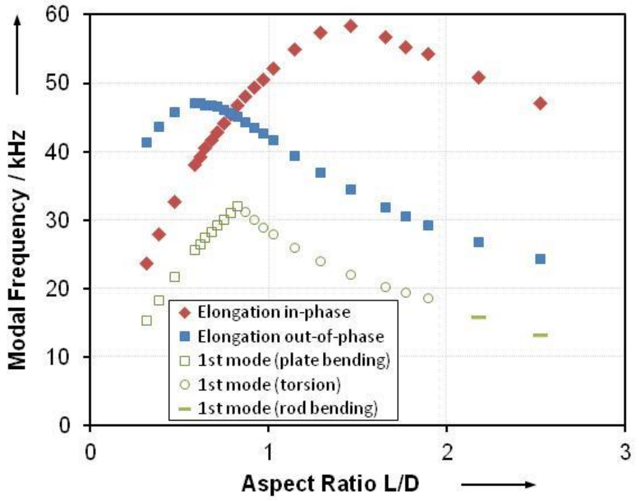

Figure 11. FE calculation of the first modal frequencies of a 1 kg cylinder made of steel in dependency of its aspect ratio length to diameter.

The previous FE calculations describe the resonances of a cylinder made of steel. The influence of the material can be estimated from the analytical solutions of the longitudinal vibrations of an elastic rod. Considering a cylindrical body of constant mass and aspect ratio, its resonance frequencies f_e depend on the material's density ρ and the modulus of elasticity E – the Poisson's ratio is assumed to be fixed, and it holds the proportionality $f_e \propto E^{1/2} \cdot \rho^{-1/6}$. To maximize the resonance frequencies of a given mass, the modulus of elasticity should be as high as possible. Compared with the material stainless steel (density about 7.9 g/cm^3), the resonances of aluminium (2.7 g/cm^3) and brass (8.4 g/cm^3) are estimated to be 30 % lower, tungsten alloy (18 g/cm^3) is almost 20 % higher, and the non-oxide ceramics silicon nitride (3.2 g/cm^3) is even 70 % higher. Steel seems to be a good choice for a metallic material, however, the exotic materials tungsten alloy and silicon nitride may be considered for special needs.

In future, the research will continue to investigate and optimize the presented experimental set-ups for the dynamic calibration of impact hammers as well as the mathematical procedures for data analysis and uncertainty estimation. This work will have to consider the calibration methods based on the time domain and the frequency domain analysis as well.

6. REFERENCES

[1] D.J. Ewins, Modal testing; theory, practice and application, 2nd ed., Research Studies Press, 2000.

[2] M. Kobusch, S. Eichstädt, L. Klaus and T. Bruns, Investigations for the model-based dynamic calibration of force transducers by using shock excitation, ACTA IMEKO, 4 (2), pp. 45–51, 2015. DOI: 10.21014/acta_imeko.v4i2.214

[3] L. Klaus, T. Bruns, H. Volkers, Calibration of bridge-, charge- and voltage amplifiers for dynamic measurement applications, Metrologia, vol. 52 (1), pp. 72-81, 2015. DOI: 10.1088/0026-1394/52/1/72

[4] International Standard ISO 16063-13:2001 Primary shock calibration using laser interferometry.